Global tropical cyclones and European windstorms in recent decline

Mark A. Saunders & Adam S. Lea

Department of Space and Climate Physics, University College London, Holmbury St Mary, Dorking, Surrey RH5 6NT, UK

Global tropical cyclones and European windstorms (strong extratropical cyclones) are the main cause of great weather disasters worldwide[1] but low confidence exists in the quantification and attribution of trends in these storms[2-7]. This uncertainty is caused by limitations in the quality and quantity of historical data, by the presence of large year-to-year variability in storm counts and by an incomplete understanding of the mechanisms that cause trends[2,4,7,8]. Here we reduce this uncertainty by clarifying the nature, significance and underlying causes of trends in these storms for the recent 1971 to 2010 period of generally sound surface windspeed data. We find that global tropical cyclones and European winter extratropical storms have been declining in annual frequency and accumulated wind power since the early 1990s; most trends for the periods 1981 to 2010 and 1991 to 2010 are significantly downward. We attribute the recent significant decline in global tropical cyclone activity to a trend towards colder ENSO (El Niño Southern Oscillation) conditions that produces anomalous zonal flows which tend to inhibit storm spin-up in the North Pacific. We attribute the recent significant decline in UK and European winter windstorm activity to a decrease in North Atlantic tropospheric thermal wind linked to warmer winter air temperatures at polar and subpolar latitudes. Despite global temperatures rising by about 0.5°C between 1971 and 2010 (refs. 9-11) our results suggest that a warming climate has had no discernible positive impact on either globally averaged tropical cyclone activity or on European extratropical cyclone activity; indeed global warming may

be contributing to the recent decrease in European strong extratropical storm activity.

Tropical cyclones and European windstorms are severe storms occurring in the tropics, subtropics and extratropics. They are characterised by damaging winds and are accompanied often by high rainfall and a coastal storm surge. Determining the nature, significance and cause of recent trends in the annual frequency and accumulated wind power of global tropical cyclones and European extratropical cyclones will improve our understanding of the long-term natural variability of these storms, assist the detection and attribution of changes in this activity due to anthropogenic climate change, and aid the forecasting of future severe storm activity.

Our analysis employs wind data sets for the 40-year period 1971 to 2010. For tropical cyclones worldwide we use track and intensity data from the International Best Track Archive for Climate Stewardship (IBTrACS) version v03r03 released in July 2011 (ref. 12). IBTrACS is a World Meteorological Organisation (WMO) data resource and contains the most complete and homogenous set of global historical tropical cyclone data currently available. We employ IBTrACS 1-minute average winds at 10m height every 6 hours (see Methods Summary for further information). For European and UK strong extratropical cyclones we use 10-minute average wind data at 10m height from the National Center for Environmental Prediction/National Center for Atmospheric Research (NCEP/NCAR) reanalysis[13]. These data are recorded every 6 hours on a 2.5° latitude by longitude grid, and are analysed for the areas 30°N-70°N, 20°W-40°E (Europe) and 50°N-60°N, 7.5°W-0°W (UK). Employing wind data from the European Centre for Medium-Range Weather Forecasts ERA40 reanalysis[14] gives almost identical results to using NCEP/NCAR reanalysis data.

The frequency of global tropical cyclones is referenced by the annual numbers of worldwide tropical storms, worldwide hurricane-strength storms and worldwide major hurricane-strength storms. These storm categories are defined respectively as having 1-

minute sustained windspeeds at 10m height of at least 63 km/h, 119 km/h and 178 km/h. The annual wind power of worldwide tropical cyclones is referenced by the global Power Dissipation Index (PDI)[15]. The frequency of European and UK strong extratropical cyclones is referenced by the number of days over the winter storm season, and for the defined area, where the 10-minute average windspeed at 10m height reached certain force levels on the Beaufort Wind Scale/WMO windspeed classification. The chosen levels are 'strong gale' force (Beaufort Scale 9, 75-88 km/h) and 'storm' force (Beaufort Scale 10, 89-102 km/h). The wind power of European and UK windstorms is referenced by the Accumulated Wind Power Index (AWPI) defined as the sum of the cubes of 6-hourly 10-minute windspeeds (in units of knots) over all 2.5° lat/long grid cells (over the defined areas) for the winter season.

Figure 1 displays the time series and linear trends for the annual incidence and wind power of global tropical cyclones and European winter extratropical cyclones. The latter are computed for the 6-month winter season from 1st October to 31st March. Linear trends are shown separately for the periods 1971-2010, 1981-2010 and 1991-2010. Four measures are provided for global tropical cyclone activity: the annual worldwide numbers of tropical storms, hurricanes, and major hurricanes and the annual global PDI. Two measures are displayed for European extra-tropical cyclone activity: the annual number of days across Europe where the 10-minute windspeed reached 'storm' force 10, and the annual AWPI over Europe. Time series are displayed for the period 1971-2010 except for the number of global major hurricanes and the global PDI which are shown only for the period 1991-2010. This is because these data are unreliable in the 1970s and 1980s due to global major hurricane numbers being inhomogeneous and under-reported during these decades (see Supplementary Information).

Figure 1 shows that global tropical cyclones and European winter extratropical storms peaked in annual frequency and accumulated wind power in the early 1990s.

Little trend is apparent over the full 1971-2010 period but trends are downward over the recent 1981 to 2010 and 1991 to 2010 periods. Table 1 displays the sign, significance and magnitude of the linear trends in Figure 1 and for two further measures of European strong extratropical cyclone activity: the number of UK wind force 9 days and the UK AWPI. The 'trend description' in Table 1 conveys the trend sign (using colour) and the confidence-in-trend (using terminology employed by the Intergovernmental Panel on Climate Change[16] to communicate uncertainty). This information combined with the trend magnitudes and trend P-values shows that reductions of over 20% have occurred for several extreme wind types over the past two or three decades and that the downward trends have become increasingly significant. For the period 1981 to 2010 most trends are significant to a P-value of 0.1, while for the period 1991 to 2010 most are significant to a P-value of 0.05.

We now examine physical explanations for the recent significant declines in global tropical cyclones and European extratropical cyclones. We start with global tropical cyclones and focus on environmental fields over the Northwest Pacific. IBTrACS data shows this basin contributes 42% of the global PDI 1991-2010, the most of any basin worldwide. Figure 2a displays the composite difference in monthly-weighted annual sea surface temperature (SST) and monthly-weighted annual 925-hPa vector winds between subset years when the global PDI 1991-2010 is in its lowest and highest quartiles. The monthly-weights are by normalised monthly global PDI contribution 1991-2010. As the figure highlights the environmental field anomalies linked to low global tropical cyclone activity, the underpinning role of La Niña ENSO in causing such activity is clear. The white rectangle in Figure 2a elucidates the physical mechanism. It marks the Northwest Pacific area of anomalous stronger trade winds, ENSO u_{trade}, associated with the anomalous zonal gradients in SST caused by La Niña. These stronger trade winds produce lower cyclonic vorticity over the Northwest Pacific region where tropical cyclones form and track. The reduced cyclonic vorticity hinders

the spinning up and intensification of storms leading to fewer tropical cyclones and a lower PDI in this basin. With La Niña also reducing tropical cyclone activity in the Northeast Pacific[17], and the North Pacific contributing 55% of the global PDI, concomitant reductions are seen in annual global tropical cyclone numbers and PDI that are linked significantly to ENSO u_{trade}. This mechanism is supported by the ENSO u_{trade} time series and its linear trends (Figure 2b) which show qualitative similarity to those in Figure 1 (a-d), and by the strength and significance of the links between ENSO u_{trade} and global and North Pacific tropical cyclone numbers and PDI (Table 2A). The *P*-values for these links are ≤0.03 for global numbers and PDI, and <0.001 for North Pacific numbers and PDI. The links with ENSO u_{trade} exceed those with the sea temperature-based Oceanic Niño Index (ONI) employed in operational definitions of ENSO[18] (Table 2A).

We next suggest a physical explanation for the recent significant decline in European strong extratropical cyclones. These cyclones gain their energy from the potential energy of the mean flow. The latter is proportional to the meridional (south-north) temperature gradient, which in turn is proportional to the vertical wind shear via thermal wind balance[19]. Thus a weaker northward gradient in air temperature implies a weaker thermal wind and lower vertical wind shear, and less potential energy for cyclone occurrence and growth. We explore the merits of this explanation for the recent decline in European extratropical cyclones. First we display (Figure 2c) the composite difference in December-February air temperature, by latitude and altitude over the extratropical and subpolar North Atlantic sector 80-0°W, between subset years when the European AWPI 1991-2010 is in its lowest and highest quartiles. As this figure highlights the temperature patterns linked to low AWPI, the significance of warming subpolar and polar air temperatures and a decreased meridional temperature gradient are evident. Our analysis next computes the zonal thermal wind, $u_{thermal}$, using the regions 30-50°N, 80-0°W and 60-80°N, 80-0°W, height integration between 1000 and 200 hPa

(the Earth's surface to upper troposphere), and NCEP/NCAR air temperature data. The $u_{thermal}$ time series and its linear trends (Figure 2d) show close similarity to those in Figure 1 (e-f). Furthermore Table 2B shows that $u_{thermal}$ is linked strongly ($r_{rank} \sim 0.8$), stably, and significantly ($P < 0.001$) to European and UK AWPI. These links match those between the North Atlantic Oscillation (NAO)[20] and European and UK AWPI. Our findings suggest strongly that the recent significant decline in UK and European winter windstorm activity is associated with a decrease in North Atlantic tropospheric thermal wind linked to warmer winter air temperatures at polar and subpolar latitudes. Our analysis does not identify the cause of the high latitude winter temperature warming in this sector, but the decline in arctic sea ice extent since the early 1990s is a potential contributory factor[21-23].

Global temperatures rose by 0.5°C between 1971 and 2010. Despite this sizeable warming no discernible positive impact of climate change is seen on either global averaged tropical cyclone activity or on European extratropical cyclone activity. Indeed these wind extremes show significant declining trends since the early 1990s when global temperatures have been at their highest[9-11]. This would suggest either the current influence of anthropogenic greenhouse gas warming on these damaging wind extremes is small compared to that of natural climate variability, or that anthropogenic greenhouse gas warming is contributing to the recent downward trends in these extremes.

METHODS SUMMARY

The IBTrACS global tropical cyclone database is not a global reanalysis; it comprises best-track data from many sources[12]. Our analysis employs the regional IBTrACS datasets used by Maue and coworkers[24,25]. Although these datasets are state-of-the-art they will contain errors in storm intensities, especially during the 1970s before the advent of global satellite coverage.

The significance of linear trends is determined using the non-parametric Mann-Kendall (MK) statistical test with correction for serial autocorrelation[26]. For each extreme wind time series we compute the effective sample size (equation 7 in ref. 26), the MK statistic S, the variance of S corrected for sample serial autocorrelation, and a normalised test statistic Z (equation A5 in ref. 26). The probability associated with Z gives the trend *P*-value for a one-tailed test. A time series with no trend has a *P*-value of 0.5. The uncertainty in the trend magnitude is estimated by taking the extreme wind distributions as approximately normal (confirmed by the Kolmogorov-Smirnov test), shuffling the extreme wind time series with replacement to generate 10,000 random slopes, converting each of these slopes to a percentage change value, and then displaying the latter in histogram form to provide a 67% confidence uncertainty. The significances in Table 2 are computed as described in the Methods section of ref. 27.

The thermal wind is computed using equation 3.32 in ref. 19. For simplicity the temperature gradient is assumed to be meridional, and the mean temperature is taken as the average temperature of abutting pressure levels. The formula is applied to all tropospheric pressure levels (1000, 925, 850, 700, 600, 500, 400, 300, 250 and 200 hPa) in the NCEP/NCAR reanalysis data. A thermal wind is computed for each pair of adjacent pressure levels and the overall thermal wind, $u_{thermal}$, is the integration over all pressure levels.

1. Munich Re NatCatService, *Great Weather Disasters* (Munich Re, Munich 2012).

2. Knutson, T. R. *et al.* Tropical cyclones and climate change. *Nature Geoscience* **3**, 157-163 (2010).

3. Peduzzi, P., *et al.* Global trends in tropical cyclone risk. *Nature Climate Change* **2**, 289-294 (2012).

4. Ulbrich, U., Leckebusch, G. C. & Pinto, J. G. Extra-tropical cyclones in the present and future climate: a review. *Theor. Appl. Climatol.* **96**, 117-131 (2009).

5. McDonald, R. E. Understanding the impact of climate change on Northern Hemisphere extra-tropical cyclones. *Clim. Dyn.* **37**, 1399-1425 (2011).

6. Trenberth, K. E. et al. Observations: Surface and Atmospheric Change. In: *Climate Change 2007: The Physical Science Basis. Contribution of Working Group I to the Fourth Assessment Report of the Intergovernmental Panel on Climate Change*, Solomon, S. et al. (Eds). 235-336 (Cambridge Univ. Press, 2007).

7. Seneviratne, S. I. et al. Changes in climate extremes and their impacts on the natural physical environment. In: *Managing the Risks of Extreme Events and Disasters to Advance Climate Change Adaption. A Special Report of Working Groups I and II of the Intergovernmental Panel on Climate Change,* C. B. Field et al. (Eds). 109-230 (Cambridge Univ. Press, 2012).

8. Coumou, D. & Rahmstorf, S. A decade of weather extremes. *Nature Climate Change* **2**, 491-496 (2012).

9. IPCC Summary for Policymakers. In *Climate Change 2007: The Physical Science Basis. Contribution of Working Group I to the Fourth Assessment Report of the Intergovernmental Panel on Climate Change*, Solomon, S. et al. (Eds). 18pp (Cambridge Univ. Press, 2007).

10. Hansen, J., Ruedy, R., Sato, M. & Lo, K. Global surface temperature change. *Rev. Geophys.* **48**, RG4004, doi:10.1029/2010RG000345 (2010).

11. American Meteorological Society *Information Statement on Climate Change* (2012); available online at http://www.ametsoc.org/policy/2012climatechange.html.

12. Knapp, K. R., Kruk, M. C., Levinson, D. H., Diamond, H. J. & Neumann, C. J. The International Best Track Archive for Climate Stewardship (IBTrACS): Unifying tropical cyclone best track data. *Bull. Am. Meteorol. Soc.* **91**, 363-376, doi:10.1175/2009BAMS2755.1 (2010).

13. Kalnay, E., *et al*. The NCEP/NCAR 40-year reanalysis. *Bull. Amer. Meteorol. Soc.* **77**, 437-471 (1996).

14. Uppala, S. M., *et al.* The ERA-40 re-analysis. *Quart. J. R. Meteorol. Soc*. **131**, 2961-3012, doi:10.1256/qj.04.176 (2005).

15. Emanuel, K. A. Increasing destructiveness of tropical cyclones over the past 30 years. *Nature* **436,** 686-688 (2005).

16. Mastrandrea, M. D. *et al*. *Guidance Note for Lead Authors of the IPCC Fifth Assessment Report on Consistent Treatment of Uncertainties*. Intergovernmental Panel on Climate Change (IPCC) (2010); available online at http://www.ipcc.ch.

17. Kim, H.-M., Webster, P. J. & Curry, J. A. Modulation of North Pacific tropical cyclone activity by the three phases of ENSO. *J. Clim*. **24**, 1839-1849, doi:10.1175/2010JCLI3939.1 (2011).

18. Kousky, V. E. & Higgins, R. W. An alert classification system for monitoring and assessing the ENSO cycle. *Wea. Forecasting* **22**, 353-371 (2007).

19. Holton, J. R. *An Introduction to Dynamic Meteorology* (3rd Edition, Academic Press, San Diego, 1992).

20. Jones, P. D., Jónsson, T. & Wheeler, D. Extension to the North Atlantic Oscillation using early instrumental pressure observations from Gibraltar and South-West Iceland. *Int. J. Climatol.* **17**, 1433–1450 (1997).

21. Kumar, A., *et al*. Contribution of sea ice loss to Arctic amplification. *Geophys. Res. Lett*. **37**, L21701, doi:10.1029/2010GL045022 (2010).

22. Petoukhov, V. & Semenov, V. A. A link between reduced Barents-Kara sea ice and cold winter extremes over northern continents. *J. Geophys. Res*. **115**, D21111, doi:10.1029/2009JD013568 (2010).

23. Wu, Q. & Zhang, X. Observed forcing-feedback processes between Northern Hemisphere atmospheric circulation and Arctic sea ice coverage. *J. Geophys. Res*. **115**, D14119, doi:10.1029/2009JD013574 (2010).

24. Maue, R. N. Recent historically low global tropical cyclone activity. *Geophys. Res. Lett*. **38**, L14803, doi:10.1029/2011GL047711 (2011).

25. Weinkle, J., Maue, R. N. & Pielke, R. A., Jr. Historical global tropical cyclone landfalls. *J. Climate* **25**, 4729-4735 (2012).

26. Yue, S. & Wang, C. The Mann-Kendall test modified by effective sample size to detect trend in serially correlated hydrological series. *Water Resources Management* **18**, 201-218 (2004).

27. Saunders, M. A. & Lea, A. S. Seasonal prediction of hurricane activity reaching the coast of the United States. *Nature* **434,** 1005-1008 (2005).

Supplementary Information is linked to the online version of the paper.

Author Contributions M.A.S. instigated and directed the research and wrote the manuscript. A.S.L. performed the data analysis and contributed ideas.
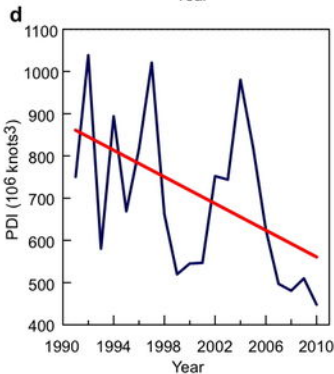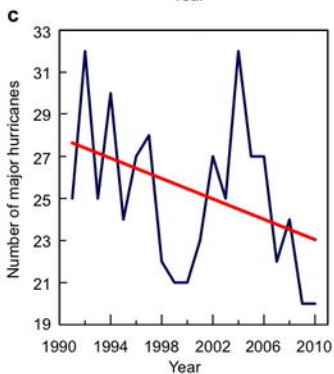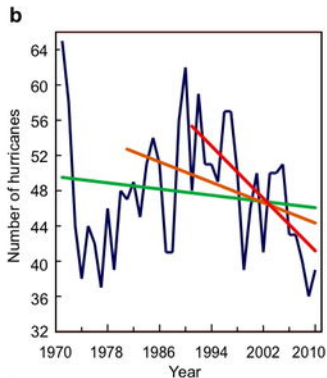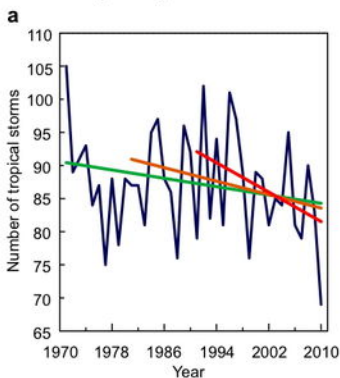
Author Information The authors declare no competing financial interests. Correspondence and requests for materials should be addressed to M.A.S. (m.saunders@ucl.ac.uk).
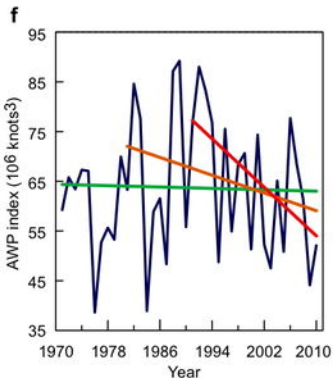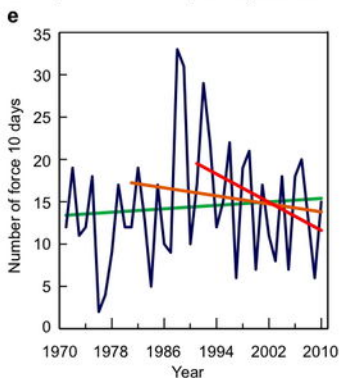
Figure Legends

Figure 1 | Nature of the trends in the frequency and wind power of global tropical cyclones and European extra-tropical cyclones between 1971 and 2010. a, b, c, d, Time series and linear trends for the annual number of global tropical storms **(a)**, global hurricanes **(b)**, global major hurricanes **(c)** and global PDI **(d)**, with **(c)** and **(d)** displayed between 1991 and 2010 only. **e, f,** Time series and linear trends for the 6-month (October to March) number of storm force days **(e)** and accumulated wind power **(f)** from extra-tropical cyclones over Europe. Colour distinguishes the trend period.

Figure 2 | Attributions for the recent significant downtrends in global tropical cyclone activity (a, b) and European extra-tropical cyclone activity (c, d). a, Annual SST (colour-coded in degrees Celsius) and 925-hPa wind anomalies (arrowed) linked to low annual global tropical cyclone activity. **b,** Time series and linear trends (colour-coded as in Figure 1) for the annual 925-hPa zonal wind u_{trade} within the white rectangular box in (**a**). **c,** December-February air temperature anomalies over the North Atlantic sector 80-0°W linked to low European winter storm activity. **d,** Time series and linear trends for the height-averaged December-February thermal wind u_{thermal} over the sector in **(c)**.

Global tropical cyclones

a Number of tropical storms vs Year

b Number of hurricanes vs Year

c Number of major hurricanes vs Year

d PDI (10^6 knots^3) vs Year

European extra-tropical cyclones

e Number of force 10 days vs Year

f AWP index (10^6 knots^3) vs Year

Linear trends: — 1971–2010 — 1981–2010 — 1991–2010

a

Latitude (°N) vs Longitude (°E)

2 m s⁻¹

-1.3 -0.9 -0.5 -0.1 0.1 0.5 0.9 1.3 (°C)

b

ENSO u_{trade} (ms⁻¹) vs Year

c

Atmosphere pressure level (hPa) vs Latitude (°N)

-3 -2 -1 0 1 2 3 (°C)
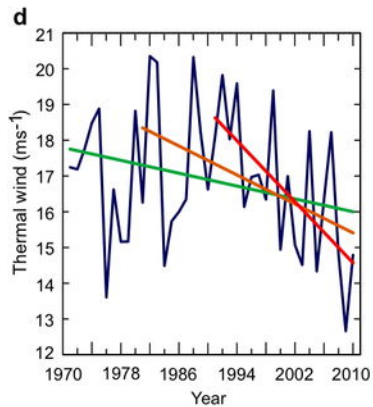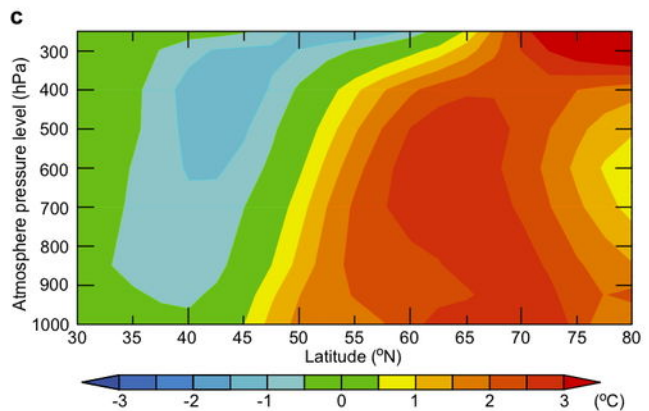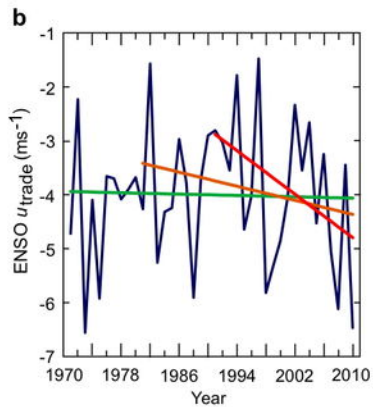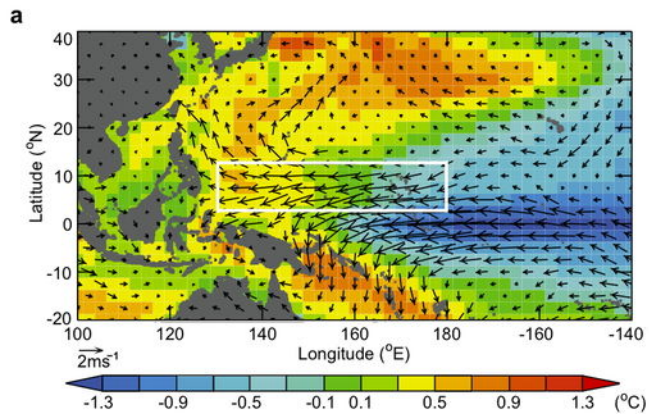
d

Thermal wind (ms⁻¹) vs Year

Table 1. Sign, significance and magnitude of recent trends in extreme wind types

Extreme wind type	Period	Trend description, significance and magnitude		
		Description	P-value	Change (%)
Global tropical storm numbers	1971-2010	Likely decreasing	0.13	-7 ± 5
	1981-2010	Likely decreasing	0.14	-8 ± 5
	1991-2010	Likely decreasing	0.16	-12 ± 8
Global hurricane numbers	1971-2010	No trend	0.38	-7 ± 9
	1981-2010	Very likely decreasing	0.07	-18 ± 7
	1991-2010	Decreasing	0.01	-30 ± 7
Global major hurricane numbers	1991-2010	Very likely decreasing	0.06	-18 ± 10
Global PDI	1991-2010	Decreasing	0.02	-44 ± 15
Europe number of wind force 10 days	1971-2010	Likely increasing	0.33	14 ± 20
	1981-2010	Likely decreasing	0.28	-24 ± 28
	1991-2010	Likely decreasing	0.13	-55 ± 30
UK number of wind force 9 days	1971-2010	Likely decreasing	0.22	-20 ± 20
	1981-2010	Decreasing	0.02	-60 ± 24
	1991-2010	Decreasing	0.03	-58 ± 30
Europe accumulated wind power	1971-2010	Likely decreasing	0.33	-2 ± 10
	1981-2010	Decreasing	0.04	-21 ± 14
	1991-2010	Decreasing	0.01	-35 ± 12
UK accumulated wind power	1971-2010	No trend	0.38	-5 ± 17
	1981-2010	Decreasing	0.05	-37 ± 22
	1991-2010	Decreasing	0.02	-49 ± 22

The trend descriptions are defined as follows: *decreasing, very likely decreasing* and *likely decreasing* mean the trend is decreasing respectively to ≥ 95% probability, ≥ 90% probability, and ≥ 67% probability; *no trend* means the trend is neither decreasing to ≥ 67% probability, nor increasng to ≥ 67% probability; *likely increasing* means the trend is increasing to ≥ 67% probability. The *P*-value gives the likelihood that the observed trend (decreasing or increasing) arises by random chance. The trend magnitude gives the percent change in the extreme wind type due to the linear trend (expressed as the most likely value ± 1 standard deviation relative to the 1971-2010 climatology (or relative to the 1991-2010 climatology for global major hurricane numbers and global PDI)).

Table 2. Links between extreme wind types and environmental fields and indices

A. Global and North Pacific tropical cyclones:

Annual extreme wind type	Period	ENSO u_{trade} annual-weighted		ENSO ONI annual-weighted	
		r_{rank}	P-value	r_{rank}	P-value
Global PDI	1991-2010	0.76	<0.001	0.68	0.001
Global MH numbers	1991-2010	0.76	0.002	0.67	0.001
Global H numbers	1991-2010	0.43	0.03	0.34	0.07
	1981-2010	0.49	0.003	0.19	0.16
	1971-2010	0.40	0.006	0.15	0.19
N. Pacific PDI	1991-2010	0.91	<0.001	0.80	<0.001
N. Pacific MH numbers	1991-2010	0.87	<0.001	0.76	<0.001
N. Pacific H numbers	1991-2010	0.78	<0.001	0.64	0.006
	1981-2010	0.73	<0.001	0.55	0.002
	1971-2010	0.63	<0.001	0.42	0.002

B. European extra-tropical cyclones:

December-February extreme wind type	Period	$u_{thermal}$ December-February		NAO index December-February	
		r_{rank}	P-value	r_{rank}	P-value
Europe accumulated wind power	1991-2010	0.80	<0.001	0.79	<0.001
	1981-2010	0.83	<0.001	0.82	<0.001
	1971-2010	0.83	<0.001	0.83	<0.001
UK accumulated wind power	1991-2010	0.78	<0.001	0.80	<0.001
	1981-2010	0.81	<0.001	0.84	<0.001
	1971-2010	0.82	<0.001	0.84	<0.001

The abbreviations are defined as follows: power dissipation index (PDI), major hurricane (MH), hurricane (H), El Niño Southern Oscillation (ENSO), Oceanic Niño Index (ONI) and North Atlantic Oscillation (NAO). The 925-hPa u_{trade} wind area is 2.5-12.5°N, 130-180°E. The $u_{thermal}$ wind area comprises latitudes 30-50°N and 60-80°N, longitudes 80-0°W and pressure levels from 1000-hPa to 200-hPa. The NAO index used is the standardised difference in mean sea level pressure between southwest Iceland and Gibraltar[20].